
Practical Applications of Constrained Form-Finding in Structural Design

Lennert LOOS^a, Kenryo TAKAHASHI^b

^aKU Leuven
lennert.loos@kuleuven.be

^bNey & Partners
kta@ney.partners

Abstract

This paper presents the application of a new form-finding method to realistic structural design case studies. The form-finding method, formulated as a constrained optimisation problem, is introduced briefly as well as the accompanying implementation as a plugin for Grasshopper[®]. Building on the authors' previous work [1] [2], the form-finding approach distinguishes itself by allowing precise control over complex geometrical constraints, steering towards a unique solution via objective functions. A meticulous control of structural geometry is often challenging with other methods, but necessary in contemporary structural design practices where form-finding is involved. The core focus of this paper is the application of the developed numerical form-finding method to realistic structural design projects, where traditional form-finding methods may fall short. The advantages and limitations of the method are discussed through a detailed discussion of three case studies of which the applied geometric constraints are explained in detail. These examples illustrate the method's effectiveness in managing complex design constraints as required in practice and bridge the gap between theory and practice, demonstrating the importance of a well-defined form-finding problem.

Keywords: Numerical Method, Form-finding, Optimisation, Geometry, Early Design Phase.

1. Introduction

In engineering design practice, designers often encounter various architectural and structural constraints that affect both geometry and structural behaviour. Traditional methods, such as the classical force density method by Schek and Linkwitz [3] or dynamic relaxation as proposed by Barnes [4] offer little flexibility in incorporating geometric constraints, hindering the exploration of the structural design space. In practice, the authors often fall back to graphic statics [5] [6] [7] as a quick and transparent way to understand form-force relationships in structural design. Drawing graphic statics diagrams, however, lacks sufficient speed for rapid feedback to gain an understanding of the degrees of freedom in the design space and the implications of altering the geometry. Manually constructing form and force diagrams of more intricate 3-dimensional networks of forces becomes a tedious task and its application is limited to planar graph topologies. In case of non-planar topologies, the graph requires a topological planarisation by cutting crossing edges and artificially reconnecting the edges [8].

Previous research by the authors elaborated on the formulation of form-finding as a constrained optimisation problem where equilibrium is imposed, and geometry and force densities are treated as concurrent variables [1] [2]. This approach allows to find discrete networks in equilibrium subjected to a single load case. The main reason for the development of this formulation can be found in the authors' desire and need to not only perform form-finding in practice whilst handling various geometrical

constraints, but also primarily to be able to work towards a specific and unique solution by means of objective functions. The objective function is crucial to find a single unique solution from the infinite amount of equilibrated solutions when the form-finding problem is under-constrained, which is often the case.

This paper focusses on the application of the form-finding method on realistic case studies, demonstrating its ability to manage geometric constraints effectively. Through these examples, the method's practical application, versatility, advantages and limitations are showcased. Besides, the case studies describe the projects' geometric constraints in detail to show the actual need in contemporary structural design projects to handle geometric constraints in a controlled way during form-finding.

2. Method

2.1. Numerical approach

The proposed method can be seen as a variation of the force density method [3], with the following key distinction from the original method: i) both nodal coordinates and force densities are used as variables, ii) the equilibrium equations, along with other geometric and force-related constraints, are considered as equality constraints in the optimization problem, iii) various objective functions are incorporated. With nodal coordinates, force densities, and reactions denoted respectively by \mathbf{p} , \mathbf{q} , and \mathbf{r} , this problem formulation can be expressed as follows.

$$\begin{aligned} & \min_{\mathbf{p}, \mathbf{q}, \mathbf{r}} f(\mathbf{p}, \mathbf{q}, \mathbf{r}) \\ & \mathbf{g}_{eq}(\mathbf{p}, \mathbf{q}, \mathbf{r}) = 0 \\ \text{s. t. } & \mathbf{g}_1(\mathbf{p}, \mathbf{q}) = 0 \\ & \vdots \\ & \mathbf{g}_n(\mathbf{p}, \mathbf{q}) = 0 \end{aligned} \quad (1)$$

Here, $f(\mathbf{p}, \mathbf{q}, \mathbf{r}) = \sum_i w_i f_i(\mathbf{p}, \mathbf{q}, \mathbf{r})$ represents the weighted summation of various objective functions, $\mathbf{g}_{eq}(\mathbf{p}, \mathbf{q}, \mathbf{r})$ the equilibrium equation (see Annex for its expression), and $\mathbf{g}_i(\mathbf{p}, \mathbf{q})$ all the other constraints. The problem (1) is then solved using sequential quadratic programming (SQP) [9] with the aid of analytical derivatives.

The most straightforward objective is least square fitting to the initial value and can be expressed by $f_{LS}(\mathbf{x}) = |\mathbf{x} - \mathbf{x}_0|^2$, where \mathbf{x}_0 is the initial value. With this objective applied to both nodal position and force density, the problem is solved for the closest fit solution in terms of numerical values of \mathbf{p} and \mathbf{q} . From a numerical point of view, the least square objective results in an identity matrix for the objective's Hessian, increasing the likelihood of the local step of SQP becoming a positive definite problem. Other objectives, such as Laplacian smoothness and soft constraints, as discussed in the paper [2] can be incorporated with different weights provide additional preferences to the solution. By default a weakly weighted least square objective function is applied with a factor of 0.001 to enhance the convergence.

This formulation allows to incorporate various constraints in form-finding, while guiding the solution towards a specific desired one through a combination of multiple objectives and corresponding weighting parameters.

2.2. Implementation of the form-finding algorithm as a parametric tool

The form-finding algorithm is integrated into the interactive CAD environment of Grasshopper® for Rhinoceros® through the development of a work-in-progress plugin written in C#. Regarding the user interface, the authors endeavoured to adhere as closely as possible to the Grasshopper® logic, aiming to create an intuitive toolbox that is adaptable to a wide range of form-finding problems. The use of the plugin is centred around form-finding models (Fig. 1) that are assembled by an equilibrium constraint, additional constraints, and one or more weighted objective functions. The equilibrium constraint is represented by a topological graph of linear elements with an initial force (density) value. In addition, information about nodal support conditions and external loads is included in the equilibrium constraint. Once a form-finding model is assembled, it can be solved in a synchronous or asynchronous way. The

asynchronous solving has the advantage of not blocking the main user interface (canvas) of Grasshopper®.

In its current state, the plugin implements various geometric and force-related constraints as shown in Figure 1: *fixed distance between nodes, equal force in elements, fixed force (density) values, keep node on line, keep node on plane, and keep node at specific position*. Three objectives are at this time implemented: stick as close as possible to the initial geometry (least square formulation), Laplacian smoothing of specific elements, and the softening of constraints. The latter “softens” a constraint by turning it into a goal or objective, rather than using it as a strict constraint.

The geometry, loads and constraints of a form-finding model (both in a solved or unsolved state) can be viewed with the model viewer (Fig. 2 left). Once a model is solved, the result viewer shows the equilibrium shape, the resulting force (density) values, and the reaction forces (Fig. 2 right).

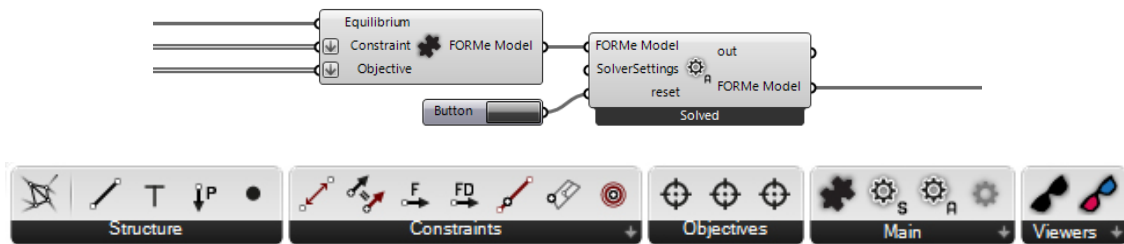


Figure 1: Assembly and solving of a form-finding model in the interactive parametric Grasshopper® environment (top). Minimalist set of Grasshopper® components that allow to assemble and solve form-finding models (bottom).

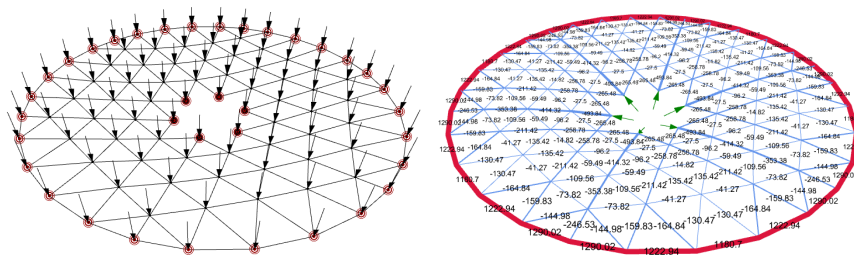


Figure 2: The unsolved form-finding model as visualised in the model viewer showing the geometry, loads and constraints (left) and the solved form-finding model as visualised with the result viewer (right).

3. Practical design applications

The following case studies display how the presented method facilitates the design process whilst being confronted with various geometrical constraints in the conception of a structural design project. For three case studies, a brief context is given and the constraints are explained in detail. Defining the form-finding problem is a nuanced task. When a limited set of geometric constraints are imposed on a form-finding problem, the geometry has flexibility to adapt and evolve in response to the problem’s requirements, but multiple solutions might be possible. Conversely, as geometric constraints become more stringent, the finding shifts towards identifying the optimal set of forces within the elements, with the geometry’s form being largely predetermined by the constraints.

3.1. 2-dimensional suspension bridge

A recent project involved a bicycle bridge, characterised by its suspension design with triangular cable configuration and a central supporting pylon that divides the bridge in two asymmetric spans. The deck of the bridge consists of discrete concrete plate segments that are post-tensioned into a continuous beam after all deck segments are installed. As shown in Fig. 3, the hangers are connected to the main cables every 5m and also every 5m to the middle of the deck segments. 40 deck segments are installed in total, 13 at one side of the pylon and 27 at the other side.

The post-tensioning of the bridge deck required the use of pendulum elements to connect the hangers to the bridge deck (Fig. 4). These pendulum elements can pivot as a way to reduce the impact of the

shortening of the deck during and after post-tensioning the entire deck (Fig. 4b). In the absence of these pendulum elements, the post-tensioning of the bridge deck would cause unwanted changes in the internal forces of the hangers, due to the shift of their longitudinal nodal positions. This is due to the static indeterminacy of the triangulated topology. Once the post-tensioning is done, the rotation of the pendulum elements is fixed (Fig. 4c).

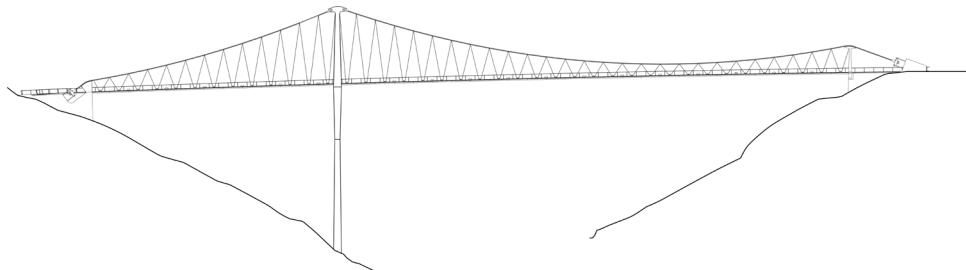


Figure 3: Elevation of the cable suspension bridge.

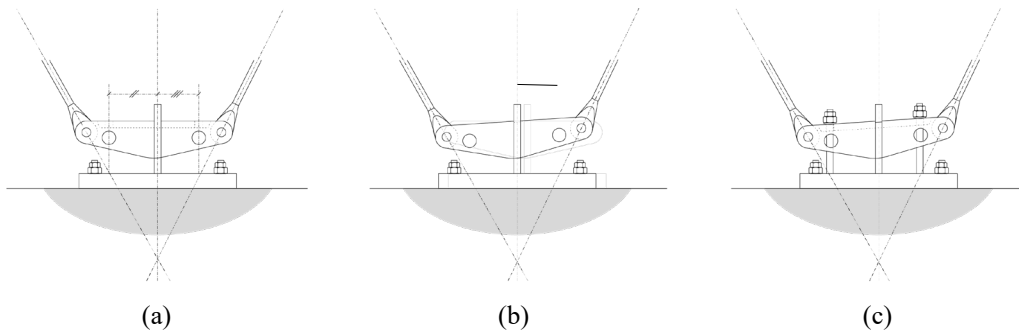


Figure 4: Concept of the pendulum design and its functioning before and after post-tensioning.

The pendulum was designed to have a fixed length of 600mm between the cable sockets. Figure 4a shows how both hangers are attached to the pendulum with slightly different angles. In order for the pendulum to be in equilibrium, the actions of the hangers must result in a net vertical force through its pivotal point. As a consequence, the pendulum cannot be positioned symmetrically in relation to the pivotal point, but an eccentricity is necessary to ensure equilibrium of the base's reaction and the cables' actions. From this description it becomes clear that determining this eccentricity of the pendulum element is not a straightforward task as it is part of the form-finding formulation.

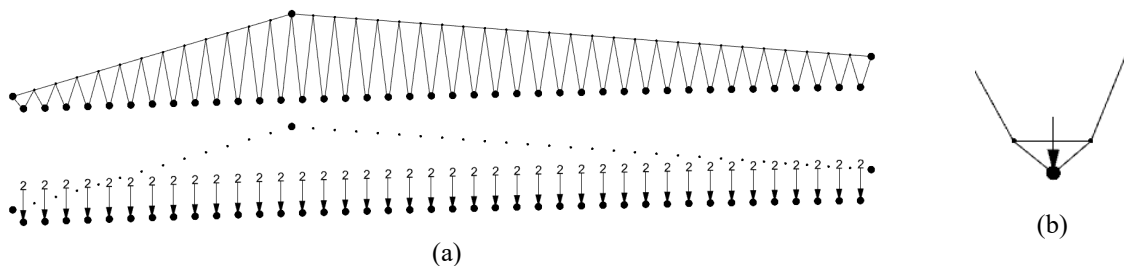


Figure 5: (a) Topological definition and initial geometry of the form-finding of the suspension bridge (left top), the applied support conditions and deck loads (left bottom). (b) A close-up of the definition of the pendulum, consisting of a horizontal pendulum bar and two elements connected to the base point. A vertical point load is applied to the pendulum bases, representing the bridge's deck load.

The initial geometry is defined by the cables (Fig. 5a). The pendulum is represented by a triangle formed by its basepoint and the two hanger ends. Figure 5b shows a close-up of the pendulum definition. The hangers have an initial force density of 1 and the main cable an initial force density of 20. The deck nodes (pendulum basepoints) are geometrically constrained and loaded with a vertical point load (value 2) representing the dead load of the deck. The nodes at the ends of the main cable are supported in all directions. The node at the top of the pylon is only supported vertically so that no horizontal load is

introduced in the pylon. The nodes of the main cable are geometrically constrained to only move vertically to keep an equal horizontal distance. The distance between the cable sockets of the pendulum bars is constrained to be 600mm and these nodes can only move horizontally. A representation of the constraints as visualised in the parametric implementation is given in Fig. 6. As the form-finding definition with this set of geometric constraints has multiple solutions, the objective function will ensure convergence towards a unique solution. The least square objective is set to keep as close as possible to the initial geometry and force density values. The force density values are chosen such that a suitable cable sag is obtained. Figure 7 shows the form-found geometry.

The presented case study gives a realistic impression of the form-finding of the suspension bridge with rather complex constraints such as the integration of the pendulums in the form-finding definition. As the set of constraints still allows for multiple solutions, the formulation of the form-finding problem as a constrained optimisation problem allows to work towards a unique solution by means of an objective function.

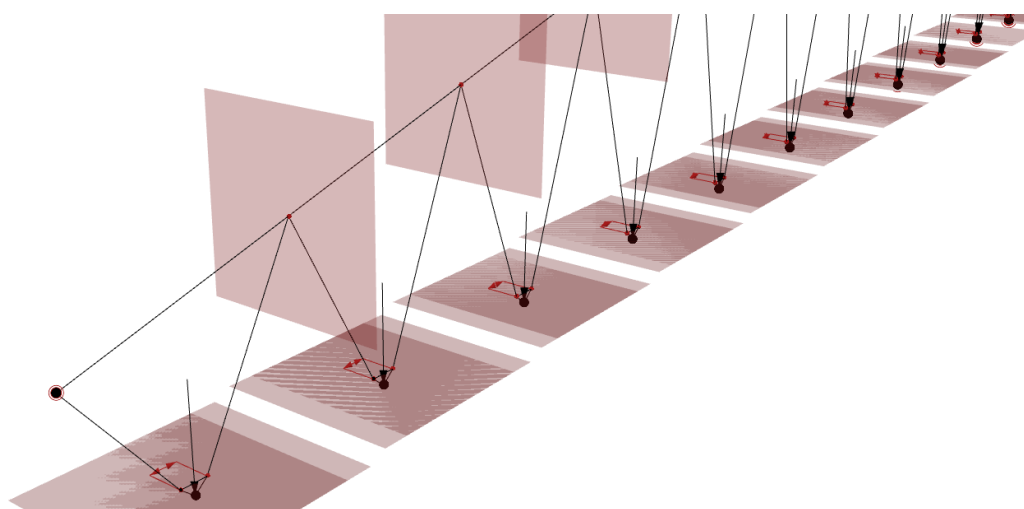


Figure 6: Visual representation of the applied constraints in the Grasshopper® environment. The top of the pendulum is initially positioned without any eccentricity and constrained onto the horizontal plane. The distance between the cable sockets of the pendulums is kept constant and the positions of the pendulum base is fixed geometrically. The nodes of the main cable can only move vertically.

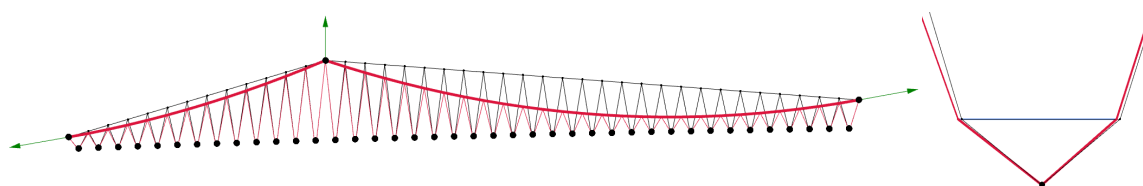


Figure 7: The initial structure (black) and the converged form-found result (red). It becomes clear that due to the fixed pendulum bases and its different cable actions, the top of the pendulum must shift slightly horizontally to find an equilibrium state. Notice as well that the action of the main cable on the pylon top is vertical as intended.

3.2. 3-dimensional self-anchored suspension bridge

This case study presents a 3-dimensional suspension footbridge of which the entire deck is geometrically defined as shown in Fig. 8. The bridge consists of 3 subspans defined by the ends of the footbridge and two sets of pylons that bear the main cables. On one side (left), the main cables are supported by two separate pylons at both sides of the deck. On the other side (right), the main cables from both sides are supported by a single pylon. The pylons' bases are coinciding with the main girders of the bridge deck, where the bridge is supported. As the bridge is a self-anchored bridge, the tension action of the main cables is taken by compression in the main girders of the bridge deck. In order to take into account both

the elevation of the deck and the in-plane bending of the deck, the entire deck is modelled as a truss and included in the form-finding formulation. The ends of the bridge deck are vertically supported and also the base of the main pylon is only vertically supported. The set of two smaller pylons are supported at their bases in all directions.

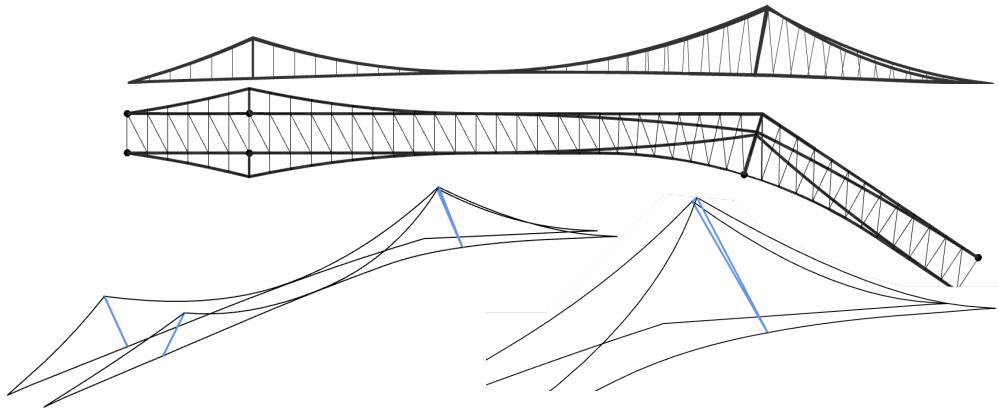


Figure 8: Elevation and plan of the suspension bridge geometry (top). Clear view on the modelling of the pylons. At the right side of the bridge, the main cables are supported by a single pylon that is modelled as a triangle to correctly model the distance between the main cables (bottom right).

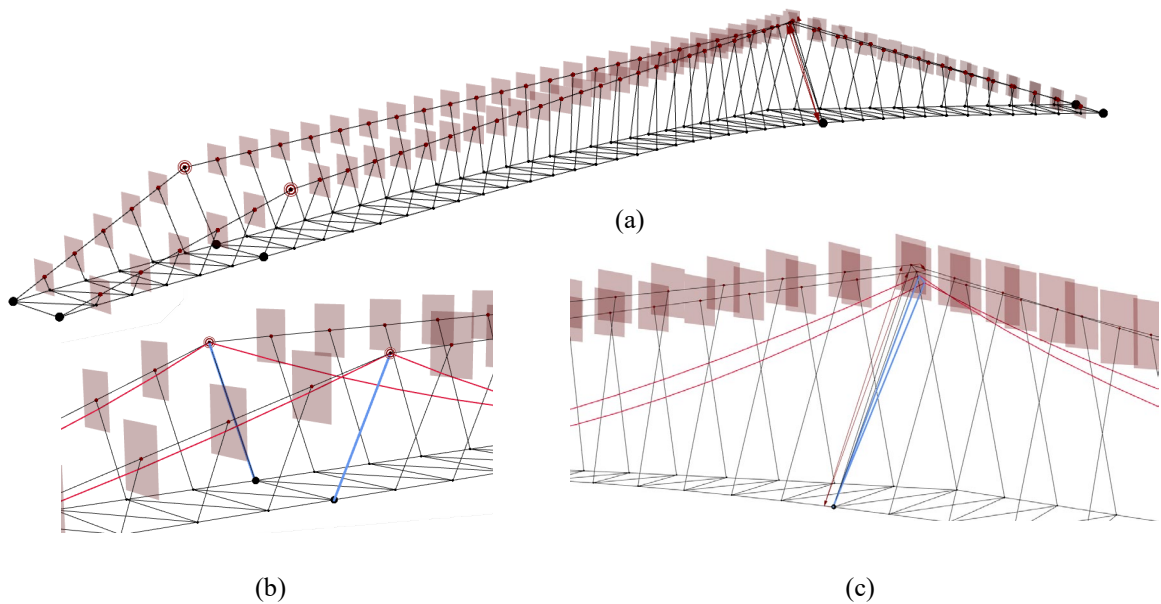


Figure 9: Overall view on the applied constraints (a). Close up of the defined constraints and the form-found result. The geometry of the deck and the small pylons is indeed maintained after form-finding (b). The triangular geometry of the main pylon is not altered after form-finding, although its orientation is different after it has found its equilibrium after form-finding (c).

At the deck nodes, a vertical load of 5 is applied and the initial force density values of the hangers is set to 5. The main cables are assigned with a positive (tension) force density value of 30, the deck girders have an initial negative (compression) force density value of -30. The other deck elements have an initial force density value of 0. The initial compression force density value of the small pylons is -15 and -8 for the main pylon. The applied constraints are the directions of the cables as their nodes should lie within planes perpendicular to the bridge's main axis (Fig. 9a). The small pylons at the left are geometrically fixed (Fig. 9b). The main pylon is modelled as a triangle and fixed in its geometry by specifying the lengths of the elements; the main pylon can only rotate in the plane perpendicular to the main bridge axis, due to the constraints applied to the nodes of the main cable (Fig. 9c). Two least square

objective functions are applied. The first one is heavily weighted by a factor 1000 and aims to maintain the geometry of the deck as much as possible. The second one, weighted by a factor 1, tries to keep the main pylon to stick close to its initial position.

Although the presented case study has got a complex set of geometric constraints and objectives, the presented method is capable of finding an equilibrium shape in a parametric environment that meets all boundary conditions. Additionally, the user interface enables a visual overview of the applied constraints. In the absence of explicit objective functions for the nodes and force densities of the main cables, the default objective is the weak (factor 0.001) least square objective applied to the nodal positions and elements' force densities. As a result, the initial force density values, as well as the nodal positions, play a primary role in the convergence towards the final solution. The force density values of the main cables are chosen in order to obtain a suitable cable sag. Figure 11 shows an example with different initial force density values for the girders and the main cables, resulting in different solutions and perhaps difficulties in convergence. In order to obtain a suitable result, good initial guesses for either the force density values or the initial nodal positions need to be provided. This requires structural knowledge and form-finding experience from the user.

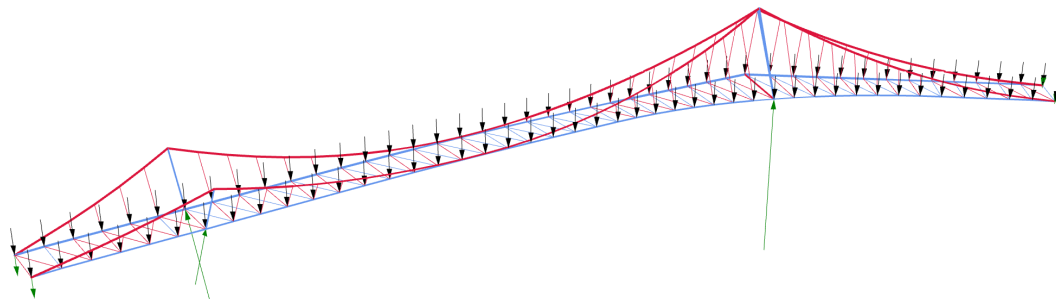


Figure 10: Resulting form-found geometry that satisfies all requested constraints and objectives. The horizontal action of the main cable ends is indeed taken by the main girders in compression. The reaction force at the main pylon is vertical as requested and the reaction forces of the smaller pylons lies in the direction of these pylons. The deck geometry has not changed after the form-finding has converged into an equilibrium shape.

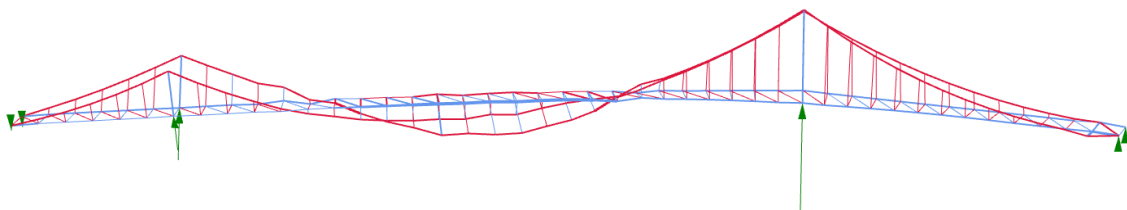


Figure 11: A non-converged result of the same form-finding problem formulation but with an initial force density value of -40 in the main girders and a force density value of 20 in the main cables. It becomes clear that the objective to keep the initial deck geometry as close as possible becomes difficult to achieve. Due to the lower force density values of the main cables, the main cable will increase in length and sag below the deck level. This results in hysteric geometry because of the needed compression in the hangers located under the deck, of which the force density values are far from the initial values. The presented result is obtained after reaching a preset maximum 1500 iterations and is not in equilibrium either.

3.3. Form-finding of a geometrically highly constrained cable net

When the set of applied geometric constraints becomes very restrictive, the geometry of the form-finding problem is mostly fixed. The majority of the free variables are the force density values in the members as most of the nodal positions are constrained. This case study searches for an equilibrated set of Y-shaped frames that are connected by pretensioned cables as shown in Fig. 12. The assembly of frames and cables form the skeleton for the mesh of an aviary enclosure. Since the end nodes of all Y-shaped frames are defined architecturally and constrained geometrically, they steer the form-finding formulation. The frames are supported at their base and the cables are supported at their ends. The central nodes of the Y-frames are free to move and the nodes where the cables form a cross are constrained to

stay within a specific vertical plane. A cable net with specific prestress needs to be found so that a self-stressed equilibrium can be achieved without compromising the frames' chosen position and orientation. A Laplacian smoothing objective, weighted with a factor 1, is applied to the geometry of the cables.

Figure 13 shows the initial form-finding model and the resulting geometry and internal forces. Due to the applied constraints, the geometry of the prestressed system has not changed much. The nodes where the cables form a cross and the central nodes of the Y-frames have changed position to ensure an equilibrated self-stressed cable net structure. The presented method is very much suited for these kinds of problems as one knows that one or more solutions exist and the number of free variables (the position of the free nodes and the force density values) is limited. Through an objective function, the method allows to work towards a unique solution.

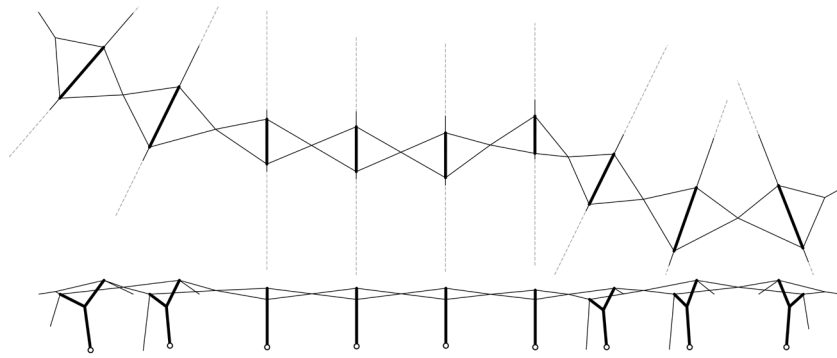


Figure 12: Plan and elevation of the pre-tensioned cable structure.

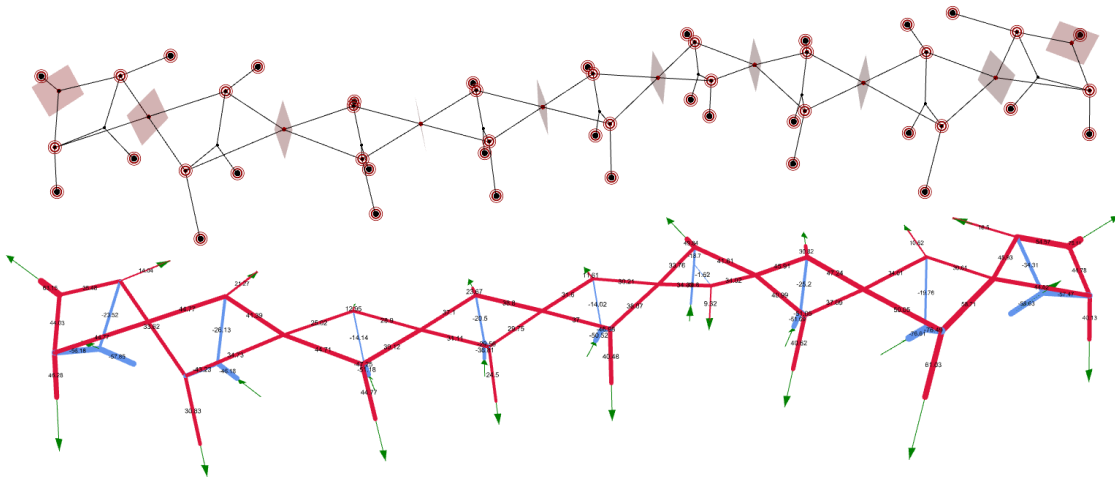


Figure 13: The form-finding model (top) is based on a given topology. All cable ends are supported, as well as the Y-shaped frames' base nodes. The position of the outer nodes of the Y-shaped frames are geometrically constrained. The initial compression force density value in the frame is set to -10. The cables have an initial force density value of 10. View of the converged form-finding model (bottom) with indication of the prestress force in the cables, compression forces in the frames, and the reaction forces.

The role of the objective function becomes clear by the example in Figure 14. In this plan view, the cable geometry of two solutions with the same constraints are shown, but with different objective functions. In one case, Laplacian smoothing is used weighted with a factor 1 as objective for the cable geometry. In the other case, a least square objective function is applied with a weighting factor 1 to the force density values of the cables. Although the geometrical differences are rather small, it shows the influence to converge towards a specific goal when multiple solutions can be found for the given constraints.

Figure 15 shows the principle of the Y-shaped frames. The presented form-finding method is based on axial member forces only. As the end nodes of the Y-shape are geometrically constrained. The shape of the Y-shape can be form-found by ensuring this central node's equilibrium and its subsequent position

(Fig. 15b). An architectural desire was to use identical symmetrical Y-shaped frames (Fig. 15c). It turned out that adding this additional constraint could not lead to a solution due to the overall plan and the shape of the cable net. This project deals with this additional constraint by making use of sufficient bending resistance of symmetrically designed frames. As long as the resultant reaction force of the frame coincides with its pinned support, equilibrium can be ensured by considering the Y-frame as a rigid body (Fig. 15c).

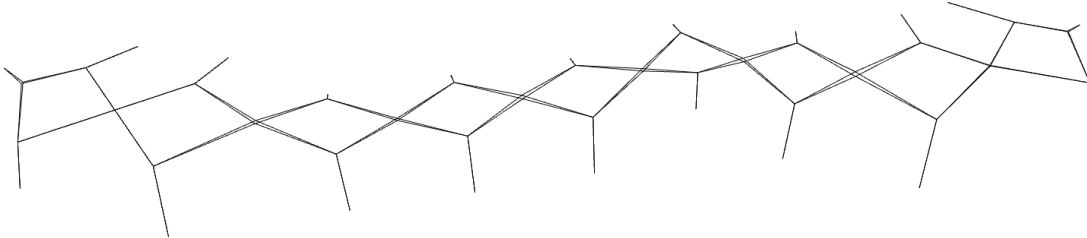


Figure 14: Objective functions allow to converge towards a specific goal and solution when multiple solutions can be found for the given constraints. Even in the highly constrained case study of the cable net, multiple solutions are possible.

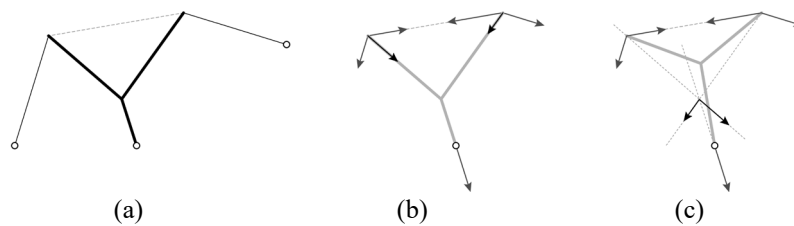


Figure 15: Overview of line model. Frames, cables, design freedom, design constraints

4. Discussion

A critical insight from the exploration is the effect of the initial force density values on the convergence of the model when the least square objective is used. In both case studies of the suspension bridges, the force density values of the main cable were chosen to obtain a suitable sag of the cable. Due to the nature of the numerical implementation, this is normal and expected behaviour, but might also influence the convergence of the entire model. The further these initial values are from the solution, the more difficult a successful convergence will be. This underscores the necessity for structural designers to possess a thorough understanding of the problem's constraints, objective functions and the ability to estimate well the force density values and the final geometry. The sensitivity to initial values when using the least square objective highlights a potential barrier for designers lacking in-depth structural intuition and experience.

From experience, the authors noticed that it is practical to gradually build up the form-finding model in terms of complexity. One starts with solving a very rudimentary form-finding model by which better initial force density values can be used later in a more complex model where more geometric constraints are applied. This approach also works when gradually refining or subdividing the geometry like in the second case study about the 2-dimensional suspension bridge with the pendulum elements.

5. Conclusion

This paper introduced a form-finding method formulated as a constrained optimisation where geometry and force densities are treated as concurrent variables while maintaining static equilibrium. Through the lens of three case studies based on real design projects, not only the application of the method is shown, but also the need for explicit geometric constraint handling in practice becomes clear through a detailed description of these constraints in a realistic design setting. The presented method showed its capability to deal with geometrical constraints effectively during form-finding. Using an objective function, the

method ensures to converge towards a unique single solution that meets all the constraints, even when multiple solutions exist that meet the set of constraints. Future research should aim to refine the method's user interface, making it more accessible to designers of varying experience levels. Furthermore, a detailed analysis of the method's convergence and a comparative study with other methods would greatly benefit the ongoing development of the presented form-finding approach.

Annex – formulation of equilibrium constraint

Compared to the original FDM, the equilibrium equation contains a minor modification through the introduction of reaction variable \mathbf{r} and can be expressed by the following.

$$\mathbf{g}_{eq}(\mathbf{p}, \mathbf{q}, \mathbf{r}) = \mathbf{C}_3^T \mathbf{Q} \mathbf{C}_3 \mathbf{p} + \mathbf{S}^T \mathbf{r} - \mathbf{f}_{ex} = \mathbf{0} \quad (2)$$

Here, \mathbf{C}_3^T , \mathbf{Q} , \mathbf{S} denotes respectively the connectivity matrix, the diagonal matrix of the vector \mathbf{q} , and the support mapping matrix. The vector \mathbf{f}_{ex} denotes the external loads. This formulation allows for separating geometric fixity and force support. Furthermore, no permutation is required to separate the fixed degrees of freedom. The advantage of using force density instead of force as variable is that the analytical derivatives can be described in a simple closed expression as follows

$$\mathbf{J}_{eq} = \begin{bmatrix} \frac{\partial \mathbf{g}_{eq}}{\partial \mathbf{p}} & \frac{\partial \mathbf{g}_{eq}}{\partial \mathbf{q}} & \frac{\partial \mathbf{g}_{eq}}{\partial \mathbf{r}} \end{bmatrix} = [\mathbf{C}_3^T \mathbf{Q} \mathbf{C}_3 \quad \mathbf{C}_3^T \mathbf{U}_3 \quad \mathbf{S}^T], \quad (3)$$

where \mathbf{U}_3 is a coordinate difference matrix.

Acknowledgement

The three case studies are adapted from projects at Ney and Partners.

References

- [1] K. Takahashi and L. Ney, 'Advanced form finding by constraint projections for structural equilibrium with design objectives', in *Proceedings of the IASS Symposium 2018*, Boston, USA, 2018.
- [2] K. Takahashi, 'Advanced form-finding with design constraints and objectives through constraint projection', in *Proceedings of the IASS Annual Symposium 2020/21 and the 7th International Conference on Spatial Structures*, Guilford, UK, 2021.
- [3] H.-J. Schek, 'The force density method for form finding and computation of general networks', *Computer Methods in Applied Mechanics and Engineering*, vol. 3, no. 1, pp. 115–134, 1974, doi: [https://doi.org/10.1016/0045-7825\(74\)90045-0](https://doi.org/10.1016/0045-7825(74)90045-0).
- [4] M. R. Barnes, 'Form Finding and Analysis of Tension Space Structures by Dynamic Relaxation', Doctoral thesis, City University London, 1977.
- [5] L. Cremona 1830-1903. and T. H. Beare, *Graphical statics; two treatises on the graphical calculus and reciprocal figures in graphical statics*. Oxford: Clarendon Press, 1890.
- [6] K. Culmann, *Die graphische Statik*. Zürich: Meyer & Zeller (A. Reimann), 1866.
- [7] J. C. Maxwell, 'XLV. On reciprocal figures and diagrams of forces', *The London, Edinburgh, and Dublin Philosophical Magazine and Journal of Science*, vol. 27, no. 182, pp. 250–261, 1864, doi: 10.1080/14786446408643663.
- [8] P. D'Acunto, J.-P. Jasienski, P. O. Ohlbrock, C. Fivet, J. Schwartz, and D. Zastavni, 'Vector-based 3D graphic statics: A framework for the design of spatial structures based on the relation between form and forces', *International Journal of Solids and Structures*, vol. 167, pp. 58–70, Aug. 2019, doi: 10.1016/j.ijsolstr.2019.02.008.
- [9] J. Nocedal and S. J. Wright, *Numerical optimization*, 2nd ed. in Springer series in operation research and financial engineering. New York, NY, USA: Springer, 2006.